Inner-shell photoionization of ground-state lithium: Theoretical calculation in the photon energy region below 130 eV including $1snln'l'$ Rydberg resonances series

L. Vo Ky,[1] P. Faucher,[1] A. Hibbert,[2] J.-M. Li,[3] Y.-Z. Qu,[3] J. Yan,[3] J. C. Chang,[4] and F. Bely-Dubau[1]
[1] *Observatoire de la Côte d'Azur, CNRS UMR No. 6529, Boîte Postale 4229, 06304 Nice Cedex, France*
[2]*Queen's University of Belfast, Belfast BT7 1NN, United Kingdom*
[3]*Institute of Physics, Chinese Academy of Science, Beijing 100080, China*
[4]*Institute of Atomic and Molecular Sciences, Academica Sinica, P.O. Box 23-166, Taipei, Taiwan 106, Republic of China*
(Received 10 September 1996; revised manuscript received 24 March 1997)

Calculations of $1s$ electron inner-shell photoionization from the $1s^22s\ ^2S^e$ Li ground state have been performed using recent developments of the *R*-matrix code with a 19-term target representation for incident photon energies up to 130 eV. This photon energy range allows important resonances in the partial cross sections due to $1snln'l'$ autoionizing states to be obtained. Theoretical resonant results are compared with recent experimental measurements of Kiernan *et al.* [J. Phys. B **29**, L181 (1996)] in the $1s2l$ threshold region. Partial cross sections, branching ratios, and asymmetry parameters are also compared outside the resonant energy range with previous theoretical results of Lisini, Burke, and Hibbert [J. Phys. B **23**, 3767 (1990)], who used the *R*-matrix code with an 11-term target representation, as well as the corresponding experimental results of Ferret *et al.* [Phys. Rev. A **36**, 3172 (1987)], Langer *et al.* [Phys. Rev. A **43**, 1652 (1991)], and Cubaynes *et al.* (private communication). [S1050-2947(98)05702-3]

PACS number(s): 32.80.Fb, 32.80.Hd

I. INTRODUCTION

The process of inner-shell photoionization of the Li atom in its ground state has been the subject of many experimental results [1–4]. High-resolution photoelectron spectra are now obtained using synchrotron radiation excitation and the experimental spectra have shown intense lines corresponding to satellite processes [5]. More recently, photoion spectra were measured at HASYLAB by Kiernan *et al.* [6], with a high-energy resolution ($E/\Delta E \simeq 10\,000$), facilitating the identification of a number of resonances, by using a dilute atomic beam of lithium crossed with monochromatized vacuum-ultraviolet synchrotron radiation. On the other hand, the important contribution of the shake-up and conjugate shake-up on the $1s$ photoionization of ground-state Li atom has stimulated theoretical investigations [7–10]. Although Li is the simplest open-shell system, the photoionization process is already complex and needs sophisticated calculations.

The purpose of the present paper is to calculate with a very-high-energy resolution the different atomic parameters that characterize the process of photoionization (partial and total cross sections, branching ratio, and β asymmetry parameter) from the $1s^22s$ ground-state Li atom, in order to reproduce the excellent experimental spectra obtained by Kiernan *et al.* at HASYLAB [6]. The calculations are performed using the *R*-matrix method as described by Berrington *et al.* [11,12] and applied to inner-shell photoionization using the practical implementation given in Vo Ky *et al.* [13]. The present paper is restricted to the photon energy range under 130 eV because in this domain a 19-term target representation is sufficient to reproduce with good quality the different experimental measurements. In a planned paper to follow, results will be extended to the hollow lithium atom with extensive calculations in the 140–165 eV photon energy range in order to reproduce the $2ln'l'n''l''$ Rydberg resonance series corresponding to l and $l'=s$ or p.

II. THEORY

The partial and total cross sections as well as the β asymmetry parameters have been calculated using the *R*-matrix method [14]. An extensive description of the *R*-matrix program and its optimization for large-scale calculation of accurate radiative atomic data has been published by Berrington *et al.* [11,12] and Seaton [15,16]. The wave function for the target plus electron is given by

$$\Psi^{SL\pi}=A\sum_{i=1}^{N^F} c_i\phi_i(S_iL_i;\mathbf{x}_1,\ldots,\mathbf{x}_N,\hat{\mathbf{x}}_{N+1})F(k_il_i;r_{N+1})r_{N+1}^{-1} + \sum_{j=1}^{N^B} d_j\Phi_j^{SL\pi}, \quad (1)$$

where the ϕ_i are the wave functions of the target terms that are included in the close-coupling (CC) expansion and are coupled to the angular and spin functions of the additional electron and $F(k_il_i;r_{N+1})$ is the radial function of the additional electron. The Φ_j in the second sum represent $(N+1)$-electron states made up entirely of target orbitals. The first term runs over all free channels N^F obtained by adding a collision-type electron with appropriate quantum numbers to the (frozen) target states, whereas the second sum includes all $(N+1)$-electron bound channels N^B (the ''bound states'') that can be made up from the target configurations plus another target orbital; this sum includes at least those configurations that have to compensate for orthogonality constraints imposed on the radial solution F and allows for the addition of correlation functions. The values N^F and N^B are depen-

dent on the mathematical model discussed below. A is the antisymmetrization operator and the coefficients c_i and d_j are determined by diagonalizing the $(N+1)$-electron Hamiltonian.

The R-matrix method has been mainly applied to electron and photon excitation of outer atomic electrons. Lisini, Burke, and Hibbert [7] used this method to analyze the various shake-up processes due to inner-shell $1s$ ionization of Li. More recently, it was extended by Vo Ky *et al.* [13] to inner-shell photoionization of Be. In this last case, although beryllium has just one more electron than lithium, a major complication in the theoretical investigation is due to the fact that the Be^+ target is a two-shell system in its lowest state $(1s^2 2s)$, whereas Li^+ is a one-shell system. The inherent problems are discussed and solved in their paper.

Photoionization calculations using the R-matrix code require the use of the same target orbitals in dealing with initial and final $(N+1)$-electron states. The choice of a good target-state (CC) expansion in the first sum of Eq. (1) as well as a good configuration-interaction (CI) expansion for each target state is very crucial. For the Li^+ target, it is only necessary to include in the CC expansion all the target states that partake in the physical processes under consideration (shake-up and conjugate shake-up). A first test of the adequacy of the CI expansions of the target states is obtained when comparing the calculated energies with experimental values. However, the most important problem to solve for the Li case concerns the selection of the $(N+1)$-electron bound states of the second sum in Eq. (1). As mentioned by Vo Ky *et al.* [13], a consistent CI selection in the $(N+1)$-electron system should retain only those $(N+1)$-electron correlation wave functions Φ_j that have corresponding parent terms in the N-electron system. A severe but good test for this crucial choice is provided by the calculation of bound states of the combined $(N+1)$-electron system. For this, a comparison of the calculated effective quantum numbers n^* with experimental values is undertaken. This test is crucial before proceeding further. In fact, the effective quantum numbers are related to bound energies of the compound system that are very close to the R-matrix poles and are very sensitive to the structure in the correlation terms describing the $(N+1)$-electron system. Any ''unbalanced'' correlation between the N- and $(N+1)$-electron systems leads, without doubt, to poor bound-state energies, i.e., bad theoretical thresholds, even starting with very reliable target states. Furthermore, this last test shows the degree of confidence in the calculation of the continuum final states of the same symmetry since the formal difference between bound- and free-state calculations depends only on their asymptotic behavior (with respect to the same target states and CI expansion included in both cases). Another good test of the CI expansion is provided by the agreement of results in the length and velocity formulations.

III. TARGET CALCULATIONS

In the present work, the CC expansion of the Li^+ target is represented by 19 states obtained from the first ten configurations $1s^2$, $1snl$, $n=2,3,4$ and $l=s,p,d,f$. The CI expansion includes up to 103 ''basic'' configurations: 54 configurations $(nln'l')$ are exclusively constituted with spectroscopic orbitals $1s,\ldots,4f$ and the 49 other configurations contain at least one nonspectroscopic orbital $5l$, $l=s,p,d,f$. With this choice of orbitals, 223 coupling configurations are used to build the 19 target states.

The target orbitals were evaluated using the code CIV3 of Hibbert [17]. The corresponding work may be considered as an extension of the previous calculations of Lisini, Burke, and Hibbert [7] in order to include the $n=4$ orbitals as ''spectroscopic'' ones and by using $5s$, $5p$, and $5d$, and $5f$ as correlation orbitals optimized on the ground state. In fact, all the radial functions are reoptimized. The differences between our $n=2$ and 3 orbital functions and those of Lisini, Burke, and Hibbert [7] are due to our choice of a 50-50 weighting of the singlet-triplet energies in the optimizations. The differences between our functions and theirs are in fact small. The orbital functions are expressed in Slater-type analytic form

$$P_{nl}(r)=\sum_{j=1}^{k} C_{jnl}\chi_{jnl}(r), \tag{2}$$

where in the Clementi-Roetti form

$$\chi_{jnl}(r)=\left[\frac{(2\zeta_{jnl})^{2I_{jnl}+1}}{(2I_{jnl})!}\right]^{1/2} r^{I_{jnl}}\exp(-\zeta_{jnl}r) \tag{3}$$

and the radial target functions satisfy the orthonormality conditions

$$\int_0^\infty P_{nl}(r)P_{n'l}(r)dr=\delta_{nn'}. \tag{4}$$

TABLE I. Method of optimization.

Orbital	Energy functional optimized
$1s$	hydrogenic $1s$ function of Li^{2+}
$2s$	$1s2s\ ^1S$ using configurations $1s^2$,$1s2s$
$3s$	average of $1s3s\ ^{1,3}S$ with configurations $1s^2$,$1s2s$,$1s3s$
$2p$	average of $1s2p\ ^{1,3}P^o$
$3p$	average of $1s3p\ ^{1,3}P^o$ with configurations $1s2p$,$1s3p$
$3d$	average of $1s3d\ ^{1,3}D$
$4s$	average of $1s4s\ ^{1,3}S$ with all configurations $msns$, $m,n\leqslant 4$
$4p$	average of $1s4p\ ^{1,3}P^o$ with all configurations $msnp$, $m,n\leqslant 4$
$4d$	average of $1s4d\ ^{1,3}D$ with configurations $1s3d$,$1s4d$,$2p^2(^1D)$,$2p3p(^{1,3}D)$
$\underline{4f}$	average of $1s4f\ ^{1,3}F^o$
$\underline{5s}$	$1s^2\ ^1S$ using all possible configurations $msns$, $m,n\leqslant 5$
$\overline{5p}$	$1s^2\ ^1S$ using configurations $1s^2+mpnp$, $m,n\leqslant 5$
$\overline{5d}$	$1s^2\ ^1S$ using configurations $1s^2+mdnd$, $m,n\leqslant 5$
$\overline{5f}$	$1s^2\ ^1S$ using configurations $1s^2$,$4f^2$,$4f\overline{5f}$,$\overline{5f}^2$

TABLE II. Radial function parameters for Li^+ target.

Orbital (nl)	C_{jnl}	I_{jnl}	ζ_{jnl}
$1s$	1.000 00	1	3.000 00
$2s$	0.706 89	1	0.980 29
	−1.566 18	2	1.017 86
$3s$	0.285 96	1	1.494 24
	−1.586 25	2	0.803 99
	1.906 56	3	0.679 72
$4s$	0.196 93	1	1.399 52
	−2.694 05	2	0.554 54
	4.687 40	3	0.586 17
	−2.705 12	4	0.498 81
$\overline{5s}$	2.823 68	1	1.672 40
	−5.930 06	2	1.816 96
	3.315 24	3	1.773 77
	−0.596 36	4	0.653 19
	0.398 20	5	0.534 56
$2p$	1.000 00	2	1.019 78
$3p$	0.983 62	2	0.830 79
	−1.535 04	3	0.647 73
$4p$	1.016 07	2	0.694 32
	−3.160 52	3	0.538 97
	2.842 05	4	0.488 58
$\overline{5p}$	1.067 81	2	4.209 53
	−0.410 20	3	1.774 15
	0.400 50	4	0.528 19
	−0.353 51	5	0.520 77
$3d$	1.000 00	3	0.666 91
$4d$	2.984 65	3	0.452 21
	−3.568 87	4	0.492 45
$\overline{5d}$	1.000 00	3	6.171 02
	−0.032 98	4	1.114 84
	0.012 17	5	0.422 35
$4f$	1.000 00	4	0.500 00
$\overline{5f}$	1.000 00	4	8.122 35
	−0.001 07	5	0.613 51

In building up the set of radial functions, we have ensured that Eq. (4) is satisfied for any P_{nl} with $n' \leqslant n$ by choosing $k = n - l$ in Eq. (2). In this way, the coefficients C_{jnl} in Eq. (2) are uniquely determined by the orthonormality conditions (4), so that (since we fix the integers I_{jnl}) only the ζ_{jnl} are treated as variational parameters.

The optimization process for each radial function is shown in Table I and the optimized parameters are shown in Table II. We included all possible angular-momentum couplings of our orbitals in the generation of the target-state functions.

The calculated target-state energies are shown in Table III, where we compare our results with experiment [18] and the earlier calculations of Lisini, Burke, and Hibbert [7]. The main difference between theory and experiment is that the $1s^2\ ^1S$ state is relatively too high in energy, i.e., not all of its correlation energy has been accounted for. However, the relative positions of the $1snl$ ($n \geqslant 2$) states are given quite well by the present calculations. Further evidence of the quality of the target-state wave functions is provided by a comparison of oscillator strengths, as presented in Table IV. Considering that our radial functions were optimized on an average of energies rather than separately on the energy of each state in the calculation, there is generally good agreement between our oscillator strengths and those of much more extensive calculations (from Weiss, quoted in [19,20]). We note that for $n \rightarrow n$ transitions, our length values are in best agreement with the accurate results, whereas for $n \rightarrow n'$ ($\neq n$) transitions, it is the velocity value that is in better agreement, a feature noted by Crossley [21]. We therefore conclude that the target-state wave functions are of sufficiently good quality for use in the present collisional calculations.

TABLE III. Target state energies relative to the $1s^2\ ^1S$ ground state of Li^+ ($E = -7.272\ 64$ a.u.). Experimental values are those given by Moore [18].

	Target state energies			
	This work		Expt. [18]	Lisini *et al.* [7]
State	(a.u.)	(cm^{-1})	(cm^{-1})	(cm^{-1})
$1s^2\ ^1S$	0	0	0	0
$1s2s\ ^3S$	2.164 10	474 965	476 046	475 209
$1s2s\ ^1S$	2.232 34	489 942	491 361	490 021
$1s2p\ ^3P^o$	2.246 48	493 046	494 273	493 087
$1s2p\ ^1P^o$	2.281 11	500 645	501 816	500 692
$1s3s\ ^3S$	2.520 17	553 113	554 761	553 460
$1s3s\ ^1S$	2.538 90	557 223	558 779	557 382
$1s3p\ ^3P^o$	2.541 90	557 882	559 501	557 966
$1s3d\ ^3D$	2.549 11	559 464	561 245	559 513
$1s3d\ ^1D$	2.549 25	559 496	561 276	559 544
$1s3p\ ^1P^o$	2.552 40	560 188	561 749	560 233
$1s4s\ ^3S$	2.635 06	578 329	579 982	
$1s4s\ ^1S$	2.642 37	579 932	581 590	
$1s4p\ ^3P^o$	2.643 56	580 194	581 897	
$1s4d\ ^3D$	2.646 42	580 821	582 612	
$1s4d\ ^1D$	2.646 50	580 839	582 631	
$1s4f\ ^3F^o$	2.646 50	580 839	582 644	
$1s4f\ ^1F^o$	2.646 50	580 839	582 645	
$1s4p\ ^1P^o$	2.647 86	581 139	582 832	

IV. TOTAL SYSTEM ($Li^+ + e$) CALCULATIONS

Initial bound states and final continuum states of the $(N+1)$-electron system are calculated on the same footing using the R-matrix method with following parameters: an R-matrix radius $a = 30.2a_0$, continuum basis functions for each orbital angular momentum $N^{\text{cont}} = 38$, and a range of orbital angular momenta of scattered electron $l \leqslant 4$. The wave function for the $(N+1)$-electron system of total symmetry $LS\pi$ is given in Eq. (1). As discussed above, the sum over Φ must include all $(N+1)$-electron states that have parent terms included in the first summation, not more, not less, and this point is crucial to obtain good energies for the $(N+1)$-electron system. Automatic procedures using Racah algebra and fractional parentage were introduced into the R-matrix code by Berrington *et al.* [12] in order to carry out the cumbersome selection process. The corresponding piece

TABLE IV. Oscillator strengths of Li^+. An asterisk denotes CI calculations of Weiss; otherwise the NBS values are obtained from the Coulomb approximation.

Transition	This work f_1	This work f_v	NBS [19]	Schiff *et al.* [20]
$1s^2\ ^1S-1s2p\ ^1P^o$	0.478	0.477	0.457*	0.457
$1s^2\ ^1S-1s3p\ ^1P^o$	0.129	0.126	0.111*	0.110
$1s^2\ ^1S-1s4p\ ^1P^o$	0.060	0.054		0.044
$1s2s\ ^1S-1s2p\ ^1P^o$	0.212	0.158	0.213*	0.213
$1s2s\ ^1S-1s3p\ ^1P^o$	0.265	0.285	0.256*	0.257
$1s2s\ ^1S-1s4p\ ^1P^o$	0.077	0.088	0.071	0.073
$1s2p\ ^1P^o-1s3s\ ^1S$	0.037	0.029	0.031	0.031
$1s3s\ ^1S-1s3p\ ^1P^o$	0.356	0.302	0.362	0.362
$1s3s\ ^1S-1s4p\ ^1P^o$	0.319	0.281	0.267	0.265
$1s2p\ ^1P^o-1s4s\ ^1S$	0.011	0.006	0.006	0.006
$1s3p\ ^1P^o-1s4s\ ^1S$	0.082	0.065	0.069	0.068
$1s4s\ ^1S-1s4p\ ^1P^o$	0.479	0.464		0.500
$1s2p\ ^1P^o-2s^2\ ^1S$	0.017	0.018		
$1s2p\ ^1P^o-2p^2\ ^1S$	0.047	0.048		
$1s3p\ ^1P^o-2s3s\ ^1S$	0.012	0.014		
$1s2s\ ^3S-1s2p\ ^3P^o$	0.326	0.357	0.308*	0.308
$1s2s\ ^3S-1s3p\ ^3P^o$	0.150	0.174	0.186*	0.187
$1s2s\ ^3S-1s4p\ ^3P^o$	0.017	0.051	0.056	0.058
$1s2p\ ^3P^o-1s3s\ ^3S$	0.034	0.042	0.039	0.039
$1s3s\ ^3S-1s3p\ ^3P^o$	0.534	0.561	0.509	0.513
$1s3s\ ^3S-1s4p\ ^3P^o$	0.134	0.170	0.189	0.189
$1s2p\ ^3P^o-1s4s\ ^3S$	0.003	0.007	0.007	0.007
$1s3p\ ^3P^o-1s4s\ ^3S$	0.072	0.081	0.085	0.085
$1s4s\ ^3S-1s4p\ ^3P^o$	0.778	0.639		
$1s2p\ ^1P^o-1s3d\ ^1D$	0.733	0.707	0.714*	
$1s2p\ ^1P^o-1s4d\ ^1D$	0.128	0.115	0.119	
$1s3d\ ^1D-1s3p\ ^1P^o$	0.014	0.019	0.016*	
$1s3p\ ^1P^o-1s4d\ ^1D$	0.689	0.642	0.654	
$1s3d\ ^1D-1s4p\ ^1P^o$	0.009	0.009	0.009	
$1s4d\ ^1D-1s4p\ ^1P^o$	0.026	0.021		
$1s2p\ ^3P^o-1s3d\ ^3D$	0.631	0.628	0.625*	
$1s2p\ ^3P^o-1s4d\ ^3D$	0.115	0.123	0.122	
$1s3p\ ^3P^o-1s3d\ ^3D$	0.092	0.067	0.090	
$1s3p\ ^3P^o-1s4d\ ^3D$	0.503	0.516	0.508	
$1s3d\ ^3D-1s4p\ ^3P^o$	0.017	0.017	0.020	
$1s4p\ ^3P^o-1s4d\ ^3D$	0.162	0.090		
$1s3d\ ^1D-1s4f\ ^1F^o$	1.018	1.016	1.02	
$1s3d\ ^3D-1s4f\ ^3F^o$	1.016	1.014	1.010	

of coding has not yet been published.

Table V gives for the two $LS\pi$ states of the $(N+1)$-electron system the number of bound terms N^B built from the 223 coupling configurations retained in the CC expansion as well as the number of channels N^{ch} that give rise to these bound terms. Note that we have $N^F = N^{ch}N^{cont}$.

TABLE V. $Li^+ + e^-$: Number of channels N^{ch} and corresponding bound terms N^B for each $LS\pi$ state.

State	N^{ch}	N^B
$^2S^e$	19	253
$^2P^o$	29	477

A. Bound states and oscillator strengths of the $Li^+ + e^-$ system

Calculated properties of the combined $Li^+ + e^-$ system test the mathematical model. The quality of the present work depends upon both a good bound ground state and continuum wave functions that are good in the whole energy range considered. An essential accuracy criterion is therefore not merely good agreement for the eigenenergy of the terms $1s^22s$ and $1s^22p$ but similar good agreement for all the higher members of the series for both the initial symmetry $^{2S+1}L^\pi = {}^2S^e$ and final symmetry $^{2S+1}L^\pi = {}^2P^o$. Table VI compares experimental and calculated effective quantum numbers for the two series $1s^2ns\ ^2S^e$ and $1s^2np\ ^2P^o$. It is seen that our results are very close to experimental ones for each series.

TABLE VI. $Li^+ + e^-$: Effective quantum numbers n^* of lithium and comparison with experimental values of Moore [18].

	$1s^2ns\ ^2S^e$		$1s^2np\ ^2P^o$	
n	Calc.	Expt.	Calc.	Expt.
2	1.588 54	1.588 53	1.959 88	1.959 38
3	2.591 86	2.596 17	2.950 73	2.955 63
4	3.597 29	3.598 35	3.956 27	3.954 40
5	4.598 40	4.599 28	4.955 78	4.953 86
6	5.599 16	5.599 77	5.955 53	5.953 21
7	6.599 60	6.599 90	6.955 39	6.953 11
8	7.599 86	7.599 58	7.955 30	7.951 64
9	8.600 03	8.599 55	8.955 24	8.953 39
10	9.600 15	9.608 18		

Another good test is also given by calculating the oscillator strengths for the combined $Li^+ + e^-$ system. Our results in the length and velocity formulations as given in Table VII are in very good agreement. They are compared, for some transitions, with Hartree-Fock calculations of Weiss [22]. Our length values agree with those of Weiss. Our velocity values differ somewhat from those of Weiss, but are in very good agreement with our length values. Our results are therefore to be preferred. The reason for the improvement over Weiss is because our procedures implicitly take core correlation more fully into account.

B. Photoionization cross sections

Partial photoionization cross sections were calculated for the process

$$1s^2 2s\ ^2S^e + h\nu \rightarrow [1snl + e(kl')]\ ^2P^o, \qquad (5)$$

where the $1snl$ configurations ($n \geq 2$) are those defined in Table III. As a typical result Fig. 1(a) shows the partial cross section for photoionization of the $1s^2 2s\ ^2S$ lithium ground state leaving the Li^+ ion in the excited state $1s2s\ ^3S$ at photon energies between 60 and 130 eV. In the low-energy range, the partial cross section is perturbed by three important series of resonances due to autoionizing states corresponding to (i) $1s2lnl'$ between 60 and 67.46 eV (the $1s2p\ ^1P$ threshold), (ii) $1s3lnl'$ between 70 and 74.83 eV (the $1s3p\ ^1P$ threshold), and (iii) $1s4lnl'$ below 77.46 eV (the $1s4p\ ^1P$ threshold). These resonances will be analyzed in Sec. IV D.

TABLE VII. $Li^+ + e^-$: gf values for transitions between $1s^2ns\ ^2S^e$ and $1s^2np\ ^2P^o$ of lithium. Comparison between length and velocity formulations. Some values calculated by Weiss [22] are also given.

	Length		Velocity	
Transition	This work	Weiss	This work	Weiss
$1s^2 2s\ ^2S - 1s^2 2p\ ^2P^o$	1.503	1.5062	1.500	1.5450
$1s^2 3s\ ^2S - 1s^2 3p\ ^2P^o$	2.443	2.4518	2.431	2.5122
$1s^2 4s\ ^2S - 1s^2 4p\ ^2P^o$	3.299		3.274	
$1s^2 5s\ ^2S - 1s^2 5p\ ^2P^o$	4.123		4.142	

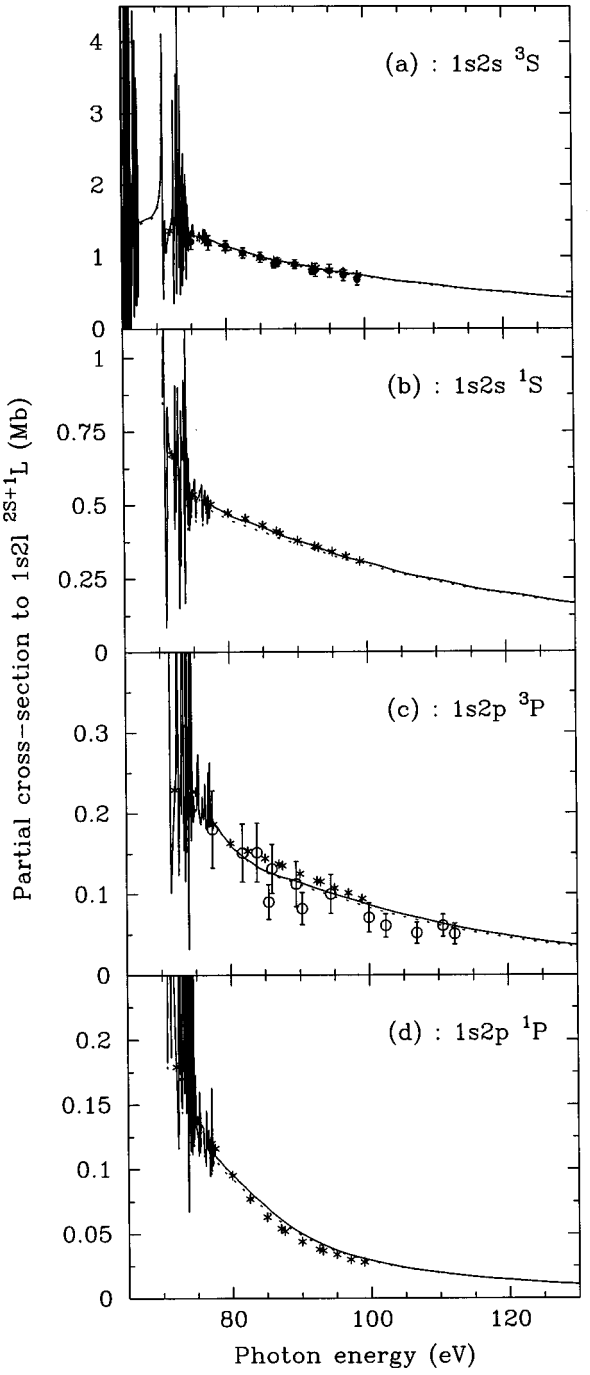

FIG. 1. Partial cross section (in megabarns) for photoionization of the $1s^2 2s\ ^2S$ lithium ground state leaving the Li^+ ion in (a) the excited state $1s2s\ ^3S$, (b) the excited state $1s2p\ ^3P$, (c) the excited state $1s2p\ ^3P$, and (d) the excited state $1s2p\ ^1P$, at incident photon energies up to 130 eV. Full line, length form; dotted line, velocity form; *, theoretical calculations from Lisini, Burke, and Hibbert [7]; ●, experimental measurements from Ferrett *et al.* [1]; ○, experimental results by Cubaynes *et al.* [23].

Extensive theoretical calculations, limited to the 72–100 eV photon energy range, have been done by Lisini, Burke, and Hibbert [7] using also the R-matrix method. In their study, the Li^+ target was represented by only 11 states built from the six first configurations $1s^2$,$1snl$ with $n \leq 3$ in their

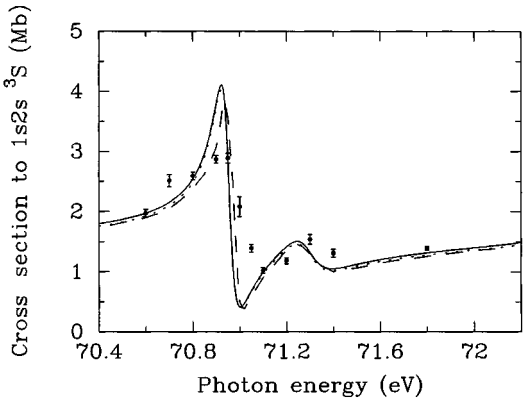

FIG. 2. Partial cross section (in megabarns) for photoionization of the $1s^2 2s\ ^2S$ lithium ground state leaving the Li^+ ion in the excited state $1s2s\ ^3S$ around the $1s3s3p\ ^3P^o$ resonance at about 71 eV. Full line, length form; dotted line, velocity form; dashed line, theoretical calculations from Lisini, Burke, and Hibbert [7]; ●, experimental measurements from Ferrett *et al.* [1] shifted by $\Delta E = -0.20$ eV.

CC expansion and adding the three pseudo orbitals $\overline{4s}$, $\overline{4p}$, and $4d$ in their CI expansion. Figures 1(a)–1(d) compare the two classes of results (11 states [7] and 19 states from the present results) with some experimental ones by Ferrett *et al.* [1] and Cubaynes *et al.* [23] for photoionization leaving the Li^+ ion in a $1s2l$ state. As it can be seen, agreement is quite good throughout the energy range. A more severe test can be made by comparing the partial photoionization cross sections leaving the Li^+ target in the $1s2s\ ^3S$ state around the $1s3s3p\ ^2P^o$ resonance at about 71 eV. Figure 2 shows very good agreement between theory and experiment around this resonance if a small shift (-0.20 eV) is imposed on the experimental energies. These first results show that an 11-state basis for the target is for the production of correct photoionization results leaving the ion in a $1s2l$ state and the agreement is yet quite good when comparing the sum of photoionization cross sections leaving the ion in any one state of the configuration $1s2l$ [Fig. 3(a)].

Agreement is not so good when comparing photoionization cross sections leaving the Li^+ ion in a $1s3l$ state. As the experimental results that are given by Ferrett *et al.* [1] are restricted to the sum of the partial photoionization cross sections leaving the ion in a $1s3l$ state, comparison will be limited to this sum and the different results are given in Fig. 3(b). At small energies the present theoretical results compare better, but are always higher than the experimental ones. The difference between the two classes of theoretical results (20% at threshold) is probably due to a better representation of the target in the present calculations.

Experimental values of the branching ratios for the shake-up and conjugate shake-up correlation satellites following $1s$ photoionization were reported previously by Ferrett *et al.* [1] and Langer *et al.* [2] in this Li $1s$ threshold region. Figures 4(a)–4(c) compare in the 72–130 eV photon energy range the present results with some of the corresponding experimental ones [1]. The comparison is quite good in the entire energy range except at higher energies for the ratio $\sigma(1s^2 2s\ ^2S \rightarrow 1s2p\ ^3P)/\sigma(1s^2 2s\ ^2S \rightarrow 1s2s\ ^3S)$. For this last ratio, another comparison is possible [Fig. 4(a)]

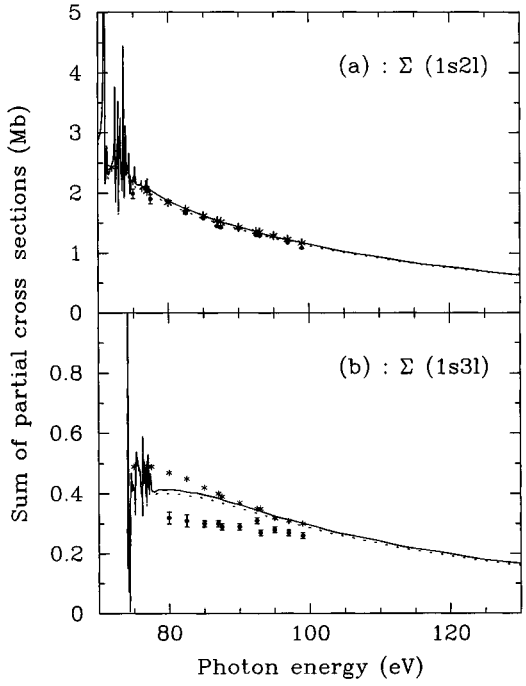

FIG. 3. Sum of the partial cross sections (in megabarns) for photoionization of the $1s^2 2s\ ^2S$ lithium ground state leaving the ion in (a) any one state of the configuration $1s2l$ and (b) any one state of the configuration $1s3l$, at incident photon energies up to 130 eV. Present results (19 states): full line, length form; dotted line, velocity form; ∗, theoretical results (11 states) of Lisini, Burke, and Hibbert [7]; ●, experimental results by Ferrett *et al.* [1].

with the more recent experimental ones measured by Cubaynes *et al.* [23]. In this last case the closer agreement with our theoretical values at high energies is due to a better precision in the measured values. Figure 5 compares the present theoretical branching ratio $\Sigma[\sigma(1s^2 2s\ ^2S \rightarrow 1s3l)]/\Sigma[\sigma(1s^2 2s\ ^2S \rightarrow 1s2l)]$ to the experimental one obtained by Ferrett *et al.* [1]. The comparison limited to the 80–100 eV photon energy range is also in good agreement.

C. The asymmetry parameter β

The asymmetry parameter β relates the differential cross section $d\sigma(L_i S_i \rightarrow L_f S_f)/d\hat{k}_f$ to the integrated cross section σ:

$$\frac{d\sigma(L_i S_i \rightarrow L_f S_f)}{d\hat{k}_f} = \frac{\sigma}{4\pi}\left[1 + \beta P_2(\cos\theta)\right], \tag{6}$$

where θ is the angle of the emitted electron measured against the polarization axis of the incident linearly polarized light. P_2 is the Legendre polynomial. To calculate the parameter, one has to add products of transition amplitudes multiplied by algebraic coefficients. Using the transfer angular momentum

$$\vec{l}_t = \vec{L}_f - \vec{L}_i = \vec{1} - \vec{l}_f, \tag{7}$$

we obtain

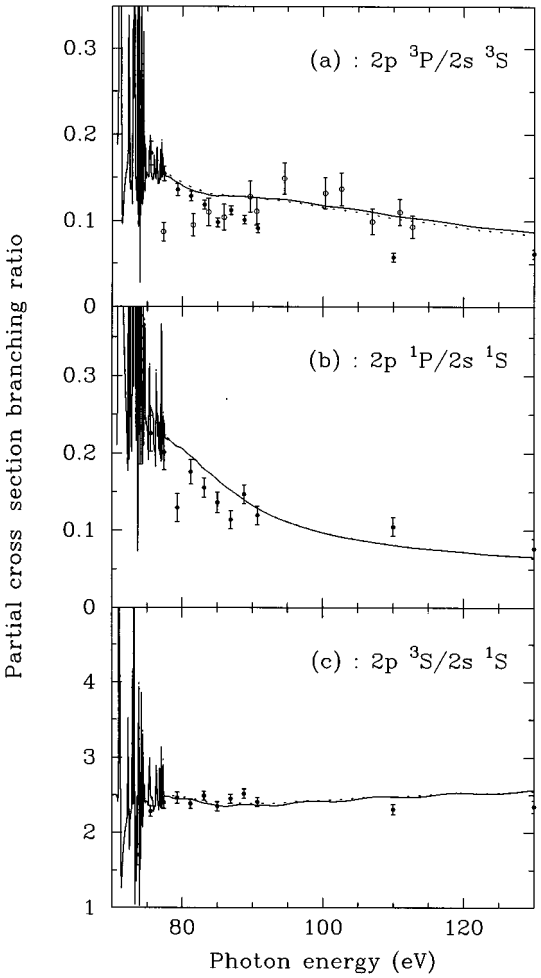

FIG. 4. Partial cross-section branching ratio: (a) $\sigma(1s^2 2s\ ^2S \rightarrow 1s2p\ ^3P)/\sigma(1s^2 2s\ ^2S \rightarrow 1s2s\ ^3S)$, (b) $\sigma(1s^2 2s\ ^2S \rightarrow 1s2p\ ^1P)/\sigma(1s^2 2s\ ^2S \rightarrow 1s2s\ ^1S)$, and (c) $\sigma(1s^2 2s\ ^2S \rightarrow 1s2s\ ^3S)/\sigma(1s^2 2s\ ^2S \rightarrow 1s2s\ ^1S)$ at incident photon energies up to 130 eV. Full line, length form; dotted line, velocity form; ●, experimental results by Ferrett *et al.* [1]; ○, experimental results by Cubaynes *et al.* [23].

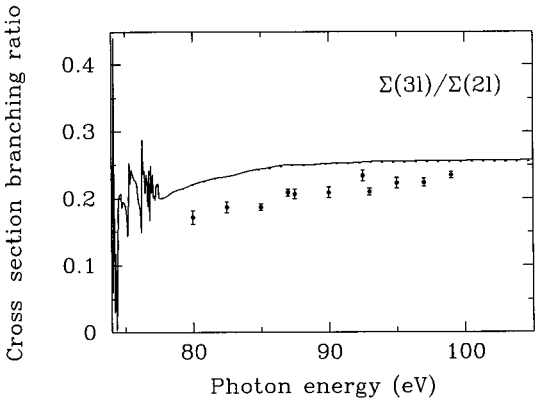

FIG. 5. Partial cross-section branching ratio $\Sigma_l \sigma(1s^2 2s\ ^2S \rightarrow 1s3l)/\Sigma_l \sigma(1s^2 2s\ ^2S \rightarrow 1s2l)$ at incident photon energies up to 110 eV. Full line, length form; dotted line, velocity form; ●, experimental results by Ferrett *et al.* [1].

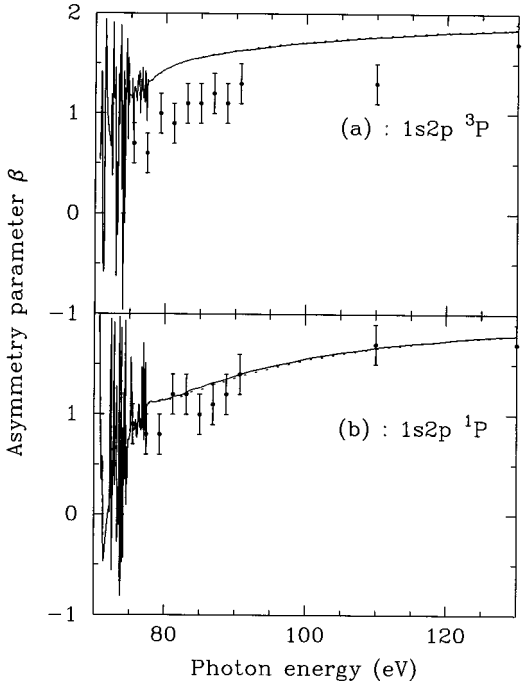

FIG. 6. Asymmetry parameter β for photoionization of $1s^2 2s\ ^2S$ lithium ground state leaving the Li^+ ion in (a) the excited state $1s2p\ ^3P$ and (b) the excited state $1s2p\ ^1P$, at incident photon energies up to 130 eV. Full line, length form; dotted line, velocity form; ●, experimental results by Langer *et al.* [2].

$$\beta(L_i S_i \rightarrow L_f S_f) = \frac{8\pi^2 \alpha a_0^2 C}{\sigma_{\rm tot}(2L_i+1)} \sum_{l_f, l_{f'}} \exp\left[-i(\sigma_{l_f} - \sigma_{l_{f'}}) + \frac{i\pi}{2}(l_f - l_{f'}) \right] ([l_f][l_{f'}])^{1/2} \langle l_f 0 l_{f'} 0 | 20 \rangle \times \langle 1010 | 20 \rangle \sum_{l_t} (-1)^{l_t} [l_t] W(1 l_f 1 l_{f'}; l_t 2) \times T^{l_t}_{L_i 1, L_f l_f} (T^{l_t}_{L_i 1, L_f l_{f'}})^*, \quad (8)$$

where

$$T^{l_t}_{L_i 1, L_f l_f} = \sum_L (-1)^L [L]^{1/2} \begin{Bmatrix} 1 & L_i & L \\ L_f & l_f & l_t \end{Bmatrix} \langle \Psi_i \| M \| \Psi_f^- \rangle,$$

$$C = \begin{cases} \omega & \text{in the length formulation,} \\ \omega^{-1} & \text{in the velocity formulation,} \end{cases}$$

$$M = \begin{cases} \sum_{j=1}^{N+1} r_j & \text{in the length formulation} \\ \sum_{j=1}^{N+1} \dfrac{\partial}{\partial r_j} & \text{in the velocity formulation,} \end{cases}$$

with the notation $[l] = (2l+1)$. The usual notation for the Clebsch-Gordan coefficients and 6-j symbols applies and the σ_l in the exponential are the Coulomb phases.

Individual partial cross sections have been distinguished experimentally by Langer *et al.* [2] and the angular-

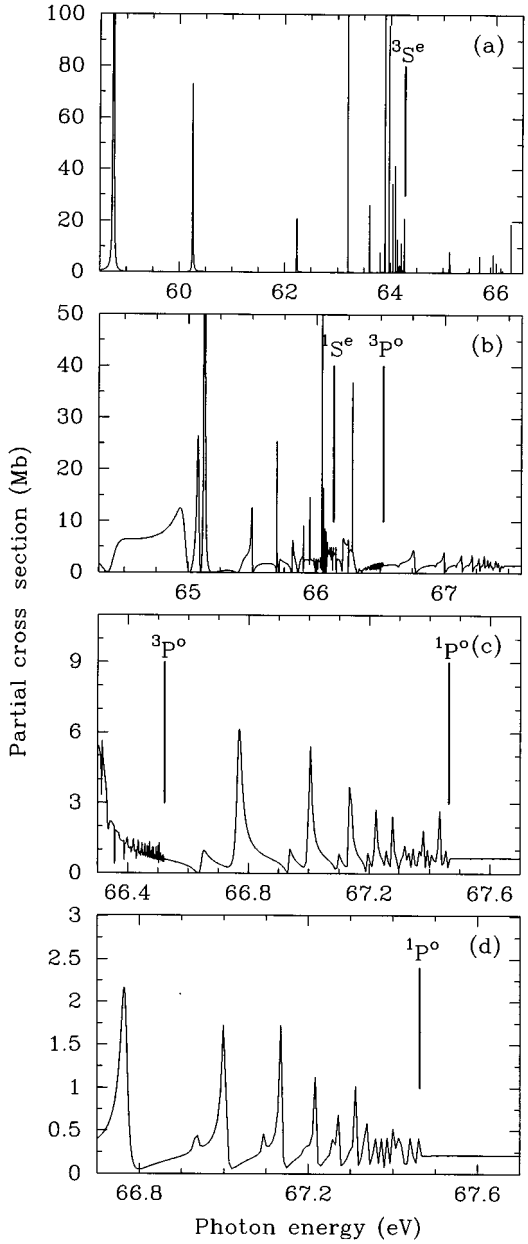

FIG. 7. Partial cross section (in megabarns) for photoionization of the $1s^2 2s\ ^2S$ lithium ground state leaving the Li^+ ion in (a) its ground state $1s^2\ ^1S$ in the photon energy region below the $1s2s\ ^3S$ threshold, (b) its excited state $1s2s\ ^3S$ in the photon energy region between the $1s2s\ ^3S$ and the $1s2p\ ^3P$ thresholds, (c) its excited state $1s2s\ ^1S$ in the photon energy region between the $1s2p\ ^3P$ and the $1s2p\ ^1P$ thresholds, and (d) its excited state $1s2p\ ^3P$ in the photon energy region between the $1s2p\ ^3P$ and the $1s2p\ ^1P$ thresholds.

distribution parameter β measured for the two conjugate shake-up satellites $1s2p\ ^3P$ and $1s2p\ ^1P$ (for the two main lines $1s2s\ ^3S$ and $1s2s\ ^1S$, $\beta=2$ as predicted by theory and confirmed by experimental results). Figures 6(a) and 6(b) compare their experimental results with the present theoretical ones in the 70–130 eV incident photon energy range where experimental measurements were done. Agreement is quite good. It is possible to obtain any asymmetry parameter from our theoretical results for any transition leaving the ion

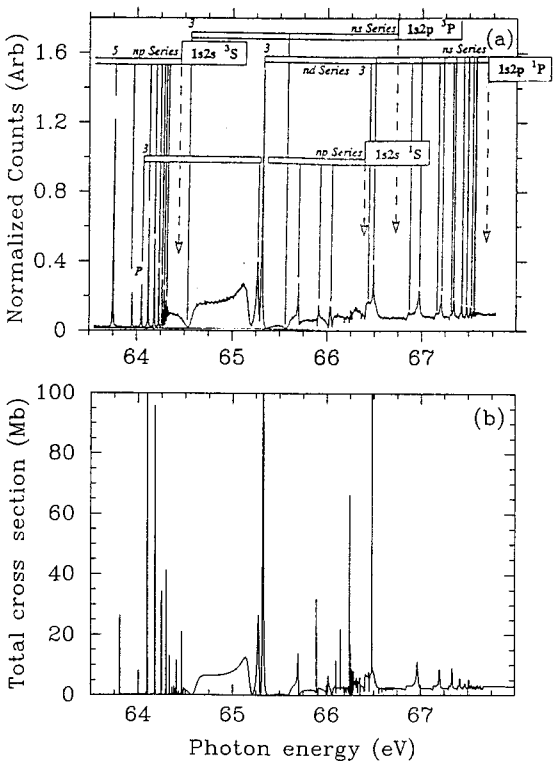

FIG. 8. Total cross section (in megabarns) for photoionization of the $1s^2 2s\ ^2S$ lithium ground state in the resonance region below the first threshold. (a) Assignment of the observed Rydberg series running to their respective limits [Ref. [6], Fig. 2(a)], and (b) present *R*-matrix calculations.

in any state given in Table III and these are available on request from the authors.

D. Resonance analysis below first and second inner-shell thresholds

Photoion spectra were recently measured with a very high spectral resolution ($E/\Delta E \simeq 10\,000$) at HASYLAB (Hamburg) by Kiernan *et al.* [6] in the 60–75 eV photon energy range. As already mentioned in Sec. IV B, this range can be divided in two important regions where we observe various Rydberg series that correspond to $1snln'l'\ ^2P$ with $n=2$ between 62 and 68 eV and $n=3$ between 70 and 75 eV, converging to first ($1s2l$) and second ($1s3l$) thresholds. Although measured partial cross sections do not exist, Figs. 7(a)–7(d) show the theoretical partial cross sections leaving the Li^+ ion respectively in the $1s^2$ ground state and in the $1s2s\ ^3S$, $1s2s\ ^1S$, and $1s2p\ ^3P$ excited states for the photon energy range of the $1s2ln'l'\ ^2P^o$ Rydberg series, as well as the position of the ionization thresholds.

The photoion technique cannot discriminate between the different partial cross sections as does in the photoelectron technique used at LSAI (Orsay, France) and described by Bizau *et al.* [24]. Comparisons between the measured Li^+ photoion yield and the *R*-matrix calculated total cross section were given by Kiernan *et al.* [6]. In the 63–68 eV photon energy range, theoretical Rydberg series converging to the $1s2l$ thresholds were previously compared with the experimental values measured by Kiernan *et al.* (see Fig. 2 in [6]).

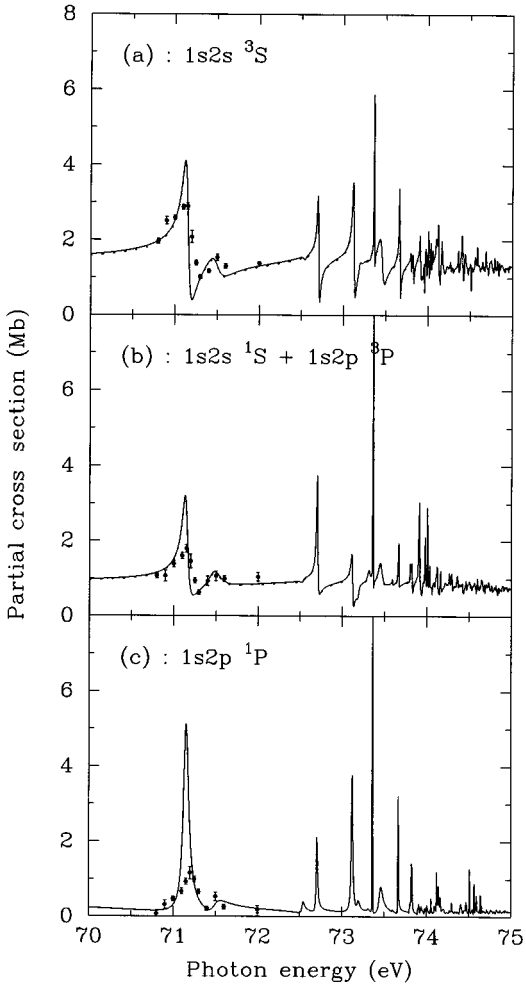

FIG. 9. Partial cross section (in megabarns) for photoionization of the $1s^2 2s\ ^2S$ lithium ground state leaving the Li^+ ion in (a) the state $1s2s\ ^3S$, (b) the states $1s2s\ ^1S$ and $1s2p\ ^3P$, and (c) the state $1s2p\ ^1P$, over the $1s3lnl'\ ^2P^o$ resonances. Full line, length form; dotted line, velocity form; ●, experimental measurements from Ferrett *et al.* [1]. Theoretical results are shifted by $\Delta E = 0.20$ eV.

As mentioned in [6], a lack of adequate intensity in the calculated spectrum for the higher members of the $[(1s2s)\ ^3S]np\ ^2P$ series is due to the density of the energy mesh used. These results were calculated with an energy mesh of 5×10^{-4} Ry (0.0068 eV). Our present calculations were performed in the energy range 63.5–67.5 eV with an energy mesh of 0.001 eV, the corresponding theoretical results for the total photoionization cross sections are compared with the measured ones in Fig. 8. These calculations reproduce well the narrow resonances of the $[(1s2s)\ ^3S]np\ ^2P$ series.

TABLE VIII. Binding energies (in eV) of the first ionization thresholds in atomic lithium: (a) *R*-matrix calculations and (b) experimental values of Moore [18].

Li^+ state	(a)	(b)	ΔE
$1s^2\ ^1S$	5.391	5.391	0
$1s2s\ ^3S$	64.276	64.410	0.134
$1s2s\ ^1S$	66.133	66.310	0.177
$1s2p\ ^3P$	66.518	66.670	0.152
$1s2p\ ^1P$	67.460	67.605	0.145
$1s3s\ ^3S$	73.965	74.169	0.204
$1s3s\ ^1S$	74.474	74.667	0.193
$1s3p\ ^3P$	74.556	74.757	0.201
$1s3p\ ^1P$	74.842	75.035	0.193

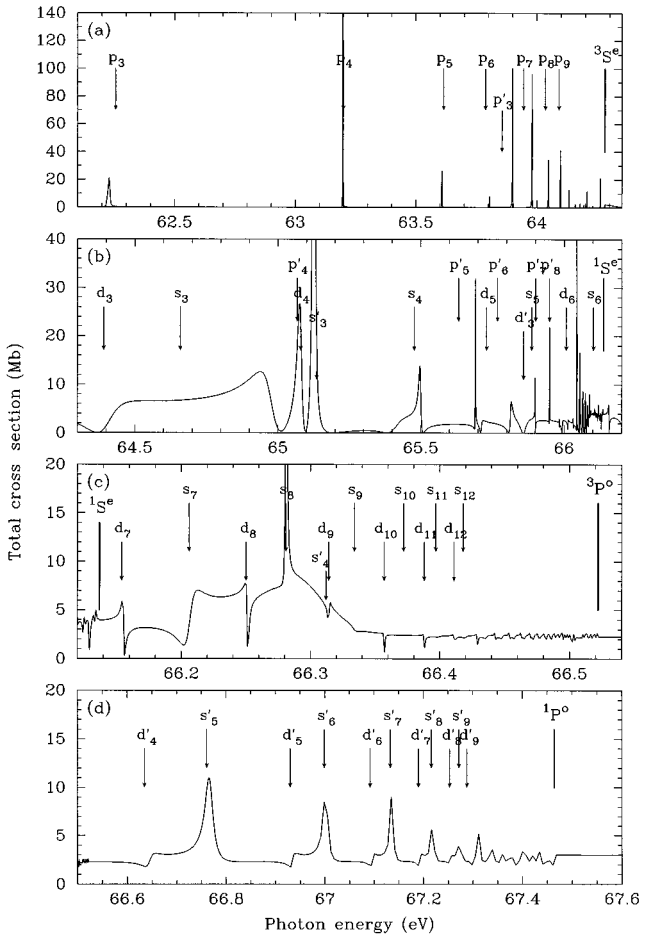

FIG. 10. Theoretical total cross section (in megabarns) for photoionization of the $1s^2 2s\ ^2S$ lithium ground state at incident photon energies (a) below the $1s2s\ ^3S$ threshold, (b) below the $1s2s\ ^1S$ threshold, (c) below the $1s2p\ ^3P$ threshold, and (d) below the $1s2p\ ^1P$ threshold. Assignment is from *ab initio* calculations using the *R*-matrix method plus MQDT [28].

In the photon energy region of the $n=3$ thresholds, agreement is quite good between the total photoionization measured by Kiernan *et al.* (Fig. 3 in [6]) and the *R*-matrix calculations. On the other hand, the strongest resonance at approximately 71.15 eV and corresponding to the $1s3s3p\ ^2P$ conjugate shake-up satellite line has also been measured by Ferrett *et al.* [1] using photoelectron spectroscopy; thus comparisons between measured and calculated partial cross sections for resonant decay to the $n=2$ states of the residual Li^+ ion are shown in Figs. 9(a)–9(c). In these figures the theoretical results that are represented for all the Rydberg series converging to $1s3l$ thresholds are shifted by 0.20 eV, taking account of the difference between theoretical and observed binding energies as given in Table VIII. Again, the agreement is quite good. It is worthwhile to note that the *ab initio* theoretical calculations should represent better the

TABLE IX. Resonance energy positions $1snln'l'\ ^2P^o$ listed in sequential form over the region of the first inner-shell thresholds. Energies quoted from the literature have been positioned according to their spectral assignment. This work (last column) represents *ab initio* calculations from the R matrix method plus MQDT [28] shifted by $+\Delta E$, where ΔE is given in Table VIII (see the text).

Label	State	Expt. [6] ($\pm$0.010 eV)	Expt. [29]	Expt. [30]	Calc. [26]	Calc. [25]	Calc. [31]	Calc. [27]	This work
				$(1s2s)\ ^3S$ threshold					
p_3	$[(1s2s)\ ^3S]3p$	62.422	62.419(3)	62.417(3)	62.424	62.436	62.280	62.418	62.386
p_4	$[(1s2s)\ ^3S]4p$	63.353	63.356(8)	63.358(3)	63.758	63.366	63.250	63.352	63.329
p_5	$[(1s2s)\ ^3S]5p$	63.752	63.753(3)	63.755(3)		63.765	63.670		63.745
p_6	$[(1s2s)\ ^3S]6p$	63.951	63.951(3)	63.956(3)		63.960			63.918
p_3'	$[(1s2s)\ ^1S]3p$	64.050	64.046(8)	64.052(3)		64.060	64.140		64.029
p_7	$[(1s2s)\ ^3S]7p$	64.121	64.121(3)	64.118(3)		64.128			64.075
p_8	$[(1s2s)\ ^3S]8p$	64.183	64.184(3)	64.181(3)		64.192			64.165
p_9	$[(1s2s)\ ^3S]9p$	64.231	64.232(6)	64.228(3)		64.241			64.221
p_{10}	$[(1s2s)\ ^3S]10p$	64.266	64.260(6)	64.258(3)		64.274			64.260
p_{11}	$[(1s2s)\ ^3S]11p$	64.292							64.288
p_{12}	$[(1s2s)\ ^3S]12p$	64.311							64.308
p_{13}	$[(1s2s)\ ^3S]13p$	64.326							64.324
p_{14}	$[(1s2s)\ ^3S]14p$	64.339							64.336
p_{15}	$[(1s2s)\ ^3S]15p$								64.346
				$(1s2s)\ ^1S$ threshold					
d_3	$[(1s2p)\ ^3P]3d$								64.536
s_3	$[(1s2p)\ ^3P]3s$	64.569			64.982				64.806
d_4	$[(1s2p)\ ^3P]4d$								65.227
p_4'	$[(1s2s)\ ^1S]4p$	65.244		65.290	65.145		65.100		65.240 s
s_3'	$[(1s2p)\ ^1P]3s$	65.289	65.250	65.238	65.254				65.282
s_4	$[(1s2p)\ ^3P]4s$	65.535		65.259	65.962				65.625
p_5'	$[(1s2s)\ ^1S]5p$	65.664		65.653	65.662		65.510		65.805
d_5	$[(1s2p)\ ^3P]5d$								65.878
p_6'	$[(1s2s)\ ^1S]6p$	65.874		65.908					65.941
d_3'	$[(1s2p)\ ^1P]3d$	66.379			65.907				66.005
s_5	$[(1s2p)\ ^3P]5s$								66.035
p_7'	$[(1s2s)\ ^1S]7p$	65.994							66.074
p_8'	$[(1s2s)\ ^1S]8p$								66.122
d_6	$[(1s2p)\ ^3P]6d$								66.155
p_9'	$[(1s2s)\ ^1S]9p$								66.183
p_{10}'	$[(1s2s)\ ^1S]10p$								66.196
p_{11}'	$[(1s2s)\ ^1S]11p$								66.211
p_{12}'	$[(1s2s)\ ^1S]12p$								66.225
p_{13}'	$[(1s2s)\ ^1S]13p$								66.236
s_6	$[(1s2p)\ ^3P]6s$								66.250
p_{14}'	$[(1s2s)\ ^1S]14p$								66.255
				$(1s2p)\ ^3P$ threshold					
d_7	$[(1s2p)\ ^3P]7d$								66.302
s_7	$[(1s2p)\ ^3P]7s$								66.354
d_8	$[(1s2p)\ ^3P]8d$								66.398
s_8	$[(1s2p)\ ^3P]8s$								66.429
s_4'	$[(1s2p)\ ^1P]4s$	66.430	66.438	66.430					66.458
d_9	$[(1s2p)\ ^3P]9d$								66.462
s_9	$[(1s2p)^3P]9s$								66.482
d_{10}	$[(1s2p)\ ^3P]10d$								66.505
s_{10}	$[(1s2p)\ ^3P]10s$								66.520
d_{11}	$[(1s2p)\ ^3P]11d$								66.536
s_{11}	$[(1s2p)\ ^3P]11s$								66.545
d_{12}	$[(1s2p)\ ^3P]12d$								66.559
s_{12}	$[(1s2p)\ ^3P]12s$								66.566

TABLE IX. (*Continued*)

Label	State	Expt. [6] (±0.010 eV)	Expt. [29]	Expt. [30]	Calc. [26]	Calc. [25]	Calc. [31]	Calc. [27]	This work
d_{13}	$[(1s2p)\ ^3P]13d$								66.576
s_{13}	$[(1s2p)\ ^3P]13s$								66.584
d_{14}	$[(1s2p)\ ^3P]14d$								66.590
s_{14}	$[(1s2p)\ ^3P]14s$								66.594
d_{15}	$[(1s2p)\ ^3P]15d$								66.601
s_{15}	$[(1s2p)\ ^3P]15s$								66.605
				$(1s2p)\ ^1P$ threshold					
d'_4	$[(1s2p)\ ^1P]4d$	66.804							66.781
s'_5	$[(1s2p)\ ^1P]5s$	66.907	66.909	66.907					66.907
d'_5	$[(1s2p)\ ^1P]5d$	67.094							67.076
s'_6	$[(1s2p)\ ^1P]6s$	67.141	67.147	67.153					67.145
d'_6	$[(1s2p)\ ^1P]6d$	67.246							67.238
s'_7	$[(1s2p)\ ^1P]7s$	67.275	67.276	67.281					67.279
d'_7	$[(1s2p)\ ^1P]7d$								67.336
s'_8	$[(1s2p)\ ^1P]8s$	67.358	67.361						67.362
d'_8	$[(1s2p)\ ^1P]8d$								67.399
s'_9	$[(1s2p)\ ^1P]9s$	67.413	67.418						67.418
d'_9	$[(1s2p)\ ^1P]9d$								67.444
s'_{10}	$[(1s2p)\ ^1P]10s$	67.453	67.459						67.457
d'_{10}	$[(1s2p)\ ^1P]10d$								67.476
s'_{11}	$[(1s2p)\ ^1P]11s$	67.477	67.482						67.485
d'_{11}	$[(1s2p)\ ^1P]11d$								67.500
s'_{12}	$[(1s2p)\ ^1P]12s$	67.502							67.506
d'_{12}	$[(1s2p)\ ^1P]12d$								67.516
s'_{13}	$[(1s2p)\ ^1P]13s$	67.516							67.521
d'_{13}	$[(1s2p)\ ^1P]13d$								67.530
s'_{14}	$[(1s2p)\ ^1P]14s$								67.534
d'_{14}	$[(1s2p)\ ^1P]14d$								67.541
s'_{15}	$[(1s2p)\ ^1P]15s$								67.544

experimental ones around the observed resonance if they were convoluted with an instrumental resolution.

E. Assignment of the resonance energy positions

As seen in Figs. 7(a)–7(d), it is sometimes difficult to assign an energy position in this complicated resonant structure. The Rydberg series associated with the $[(1s2s)\ ^3S]np\ ^2P$ configurations are observable until $n=14$ with a perturber (the $[(1s2s)\ ^1S]3p\ ^2P$ state) already detected by Chung [25] using the saddle-point technique. Likewise, the higher members of the $[(1s2p)\ ^1P]ns\ ^2P$ series are also easily identified running up to the $1s2p\ ^1P$ threshold at 67.61 eV as well as the $[(1s2p)\ ^1P]nd\ ^2P$ series that appears as a weak shoulder to the low-energy side of the $[(1s2p)\ ^1P](n+1)s\ ^2P$ resonances. Energy positions are more difficult to determine in the photon energy range between 64 and 66.7 eV.

Due to very high resolution in their observed spectra, Kiernan *et al.* [6] have been able to assign a lot of observed resonance energy positions, which various theoretical approaches had attempted to identify [7,25–27]. Identifications of the $[(1s2s)\ ^3S]np\ ^2P$ Rydberg resonances, obtained from the saddle-point technique [25,27], are very close to the observed measurements, but the assignments from the quasi-projection-operator technique [26] are less precise.

Recently, Li *et al.* [28] proposed a way to perform photoionization R-matrix calculations. The wave functions in the outer region defined in the R-matrix method are calculated directly from the logarithmic derivative of the solution at the boundary R matrix and from the physical eigenchannel parameters (quantum defects μ_α and orthogonal transformation matrix $U_{i\alpha}$) in multichannel quantum defect theory (MQDT). Such unified theory between the R-matrix method and MQDT allows us to obtain clear assignments for overlapped resonances. This method is applied to identify the $1s2ln'l'\ ^2P$ Rydberg series in the photon energy range between 62 and 67.5 eV. The present calculated results (R-matrix method plus MQDT) are given in the last column of Table IX, where all the other columns are those given in Table 3 of Kiernan *et al.* [6]. In the present calculations, energy positions were shifted by the difference ΔE as given in Table VIII for each series. For example, a shift of $\Delta E=0.134$ eV was applied to each *ab initio* energy calculation for the $[(1s2s)\ ^3S]np\ ^2P$ Rydberg series ($E_{\rm th}+\Delta E=E_{\rm obs}$).

Assignments that are given in Table IX are obtained directly from eigenphase shifts of the wave function deter-

mined outside the R-matrix box and corresponding to a channel $1s2ln'l'\ ^2P^o$. These assignments do not take account of interferences between all the states, whereas in the photoionization cross-section calculation the resonances are overlapped. These interferences can modify crucially the effective position of these resonances. This is illustrated in Figs. 10(a)–10(d), where the total photoionization cross section is respectively given below each $1s2l$ threshold. In these figures that give *ab initio* results (without any shift in energy), arrows represent assignments obtained from the last column in Table IX. In the different zones where there is no mixing between resonances, arrows give clear assignment ratifying results given in Table IX. On the other hand, when these interferences are important, we note a significant shift between calculated assignment and effective resonance position. Thus, in Fig. 10(a), the $[(1s2s)\ ^1S]3p\ ^2P$ state perturbs highly the pattern of the $[(1s2s)\ ^3S]np\ ^2P$ states around $n=7$. The interferences are more complex in the two zones below the $1s2s\ ^1S$ and $1s2p\ ^3P$ thresholds [Figs. 10(b) and 10(c)]. As it can be seen in Table IX, only some assignments were given by Kiernan *et al.* [6] in these energy ranges. In spite of strong interferences between the two series $(1s2s\ ^1P)np$ and $(1s2p\ ^3P)ns$ as shown in these figures, additional assignments can be proposed from present calculations.

V. CONCLUSION

The present R-matrix calculation includes photoionization from the ground state $1s^22s\ ^2S^e$ of neutral lithium for incident photon energies up to 130 eV. This energy range allows us to take account for resonances due to excited states corresponding to $1snln'l'$ configurations. In the R-matrix code, the CC expansion of the Li^+ target is represented by 19 states and the CI expansion includes up to 103 basic configurations. The quality of the target wave functions as well as bound and continuum ones for the $Li^+ + e$ system is proved when comparing calculated energies with experimental ones and oscillator strengths with other sophisticated theoretical calculations. This quality in the results implies an extensive and correctly balanced configuration expansion for the target and for the $(N+1)$-electron states.

Partial and total photoionization cross sections are shown in some detail. In particular, resonances due to the $1s2lnl'$ Rydberg series and most recently observed by Kiernan *et al.* [6] are well reproduced. New assignments of these resonances are possible using the theory recently developed by Li *et al.* [28]. Partial cross sections, branching ratios, and asymmetry parameters extend the previous theoretical results of Lisini, Burke, and Hibbert [7] and compare well with the experimental ones of Ferrett *et al.* [1], Langer *et al.* [2], and Cubaynes *et al.* [23].

Theoretical results are only given for transitions where, in general, a comparison was possible with experiment. Any other theoretical result for any transition towards any state given in Table III is also available upon request.

ACKNOWLEDGMENTS

The calculations were carried out partly on the CRAY YMP/2E computer at the IMT, Marseille, France (supported by the Conseil Régional Provence-Alpes-Côte d'Azur) and partly on the CRAY C98 (IDRIS France, Project No. 940052). We thank F. J. Wuilleumier's group for communicating experimental results before publication. A.H. acknowledges partial support from the EC HCM Network, Contract No. CHRX-CT93-0361.

[1] T. A. Ferrett, D. W. Lindle, P. A. Heimann, W. D. Brewer, U. Becker, H. G. Kerhoff, and D. A. Shirley, Phys. Rev. A **36**, 3172 (1987).

[2] B. Langer, J. Viefhaus, O. Hemmers, A. Menzel, R. Wehlitz, and U. Becker, Phys. Rev. A **43**, 1652 (1991).

[3] P. Gerard, D. Cubaynes, J.-M. Bizau, and F. J. Wuilleumier, J. Phys. (Paris), Colloq. **48**, C9-719 (1987).

[4] D. Cubaynes, J.-M. Bizau, F. J. Wuilleumier, B. Carré, and F. Gounand, Phys. Rev. Lett. **63**, 2460 (1989).

[5] L. Journel, B. Rouvellou, D. Cubaynes, J.-M. Bizau, and F. J. Wuilleumier, in *Proceedings of the XVIIIth International Conference on the Physics of Electronic and Atomic Collisions*, edited by Torkild Andersen, Bert Fastrup, Finn Folkmann, Helge Knudsen, and N. Andersen, AIP Conf. Proc. 295 (AIP, New York, 1993), p. 22; Bull. Am. Phys. Soc. **38**, 1139 (1993).

[6] L. M. Kiernan, M.-K. Lee, B. F. Sonntag, P. Zimmermann, J. T. Costello, E. T. Kennedy, A. Gray, and L. Vo Ky, J. Phys. B **29**, L181 (1996).

[7] A. Lisini, P. G. Burke, and A. Hibbert, J. Phys. B **23**, 3767 (1990).

[8] F. P. Larkins and J. A. Richards, Aust. J. Phys. **39**, 809 (1986).

[9] G. B. Armen, B. I. Craig, F. P. Larkins, and J. A. Richards, J. Electron Spectrosc. Relat. Phenom. **51**, 183 (1990).

[10] L. Vo Ky, A. Hibbert, L. Journel, B. Rouvellou, D. Cubaynes, J.-M. Bizau, and F. J. Wuilleumier (unpublished).

[11] K. A. Berrington, P. G. Burke, M. Le Dourneuf, W. D. Robb, K. T. Taylor, and L. Vo Ky, Comput. Phys. Commun. **14**, 367 (1978).

[12] K. A. Berrington, P. G. Burke, K. Butler, M. J. Seaton, P. J. Storey, K. T. Taylor, and Yu Yan, J. Phys. B **20**, 6379 (1987).

[13] L. Vo Ky, H. E. Saraph, W. Eissner, Z. W. Liu, and H. P. Kelly, Phys. Rev. A **46**, 3945 (1992).

[14] P. G. Burke and W. D. Robb, Adv. At. Mol. Phys. **15**, 143 (1975).

[15] M. J. Seaton, J. Phys. B **18**, 2111 (1985).

[16] M. J. Seaton, J. Phys. B **20**, 6363 (1987).

[17] A. Hibbert, Comput. Phys. Commun. **9**, 141 (1975).

[18] C. E. Moore, *Atomic Energy Levels I*, Natl. Bur. Stand. (U.S.) Circ. No. 467 (U.S. GPO, Washington, DC, 1949), Vol. I.

[19] W. L. Wiese, M. W. Smith, and B. M. Glennon, *Atomic Transitions Probabilities*, Data Ser., Natl. Bur. Stand. (U.S.) Circ. No. 4 (U.S. GPO, Washington, DC, 1966), Vol. 1.

[20] B. Schiff, C. L. Pekeris, and Y. Accad, Phys. Rev. A **4**, 885 (1971).

[21] R. J. S. Crossley, Adv. At. Mol. Phys. **5**, 237 (1969).
[22] A. W. Weiss, Astrophys. J. **138**, 1262 (1963).
[23] D. Cubaynes, J.-M. Bizau, L. Journel, B. Rouvellou, and F. Wuilleumier (private communication).
[24] J. M. Bizau, D. Cubaynes, M. Richter, F. J. Wuilleumier, J. Obert, and J.-C. Putaux, Rev. Sci. Instrum. **63**, 1389 (1992).
[25] K. T. Chung, Phys. Rev. A **23**, 2957 (1981).
[26] S. Wakid, A. K. Bhatia, and A. Temkin, Phys. Rev. A **21**, 496 (1980).
[27] M. K. Chen and K. T. Chung, Phys. Rev. A **49**, 1675 (1994).
[28] J. M. Li, L. Vo Ky, Y. Z. Qu, J. Yan, P. H. Zhang, H. L. Zhou, and P. Faucher, Phys. Rev. A **55**, 3239 (1997).
[29] D. L. Ederer, T. Lucarto, and R. P. Madden, Phys. Rev. Lett. **25**, 1537 (1970).
[30] A. M. Cantu, W. H. Parkinson, G. Tondello, and P. J. Tozzi, J. Opt. Soc. Am. **77**, 2144 (1977).
[31] A. Lisini, in *Synchrotron Radiation and Dynamic Phenomena*, edited by A. Beswick, AIP Conf. Proc. No. 258 (AIP, New York, 1992), p. 149.